JOC The Journal of Organic Chemistry

Article

pubs.acs.org/joc

2D Ultrafast HMBC $^{1}H,^{31}P$: Obtaining Mechanistic Details on the Michaelis–Arbuzov Reaction

María Encarnación Fernández-Valle,[‡] Roberto Martínez-Álvarez,[†] Dolores Molero-Vílchez,[‡] Zulay D. Pardo,[†] Elena Sáez-Barajas,[‡] and Antonio Herrera*[,‡,†]

[†]Departamento de Química Orgánica I, Facultad de Químicas, Universidad Complutense, 28040 Madrid, Spain

[‡]CAI de RMN y RSE, Facultad de Químicas, Universidad Complutense, 28040 Madrid, Spain

Supporting Information

ABSTRACT: Ultrafast NMR spectroscopy (UF-NMR) can be used to monitor chemical reactions in real time and to provide insights into their mechanisms and the nature of the intermediates formed. Here, we have developed a 2D $^{1}H,^{31}P$ UF-HMBC method and the corresponding NMR experimental setup to enable the study of a Michaelis–Arbuzov reaction at two different temperatures, 25 and 70 °C. The specific reaction studied was between triethyl phosphite and benzyl bromide to produce diethylbenzyl phosphonate. Our results show that at 70 °C the reaction takes place directly, without the detection of an intermediate by $^{1}H,^{31}P$ UF-HMBC. In contrast, at 25 °C, using zinc bromide as a catalyst, our results show the formation of benzyltriethoxy phosphonium bromide as an intermediate. The experiments again show the power of UF-NMR in mechanistic studies of reactions involving various phosphorus chemical species.

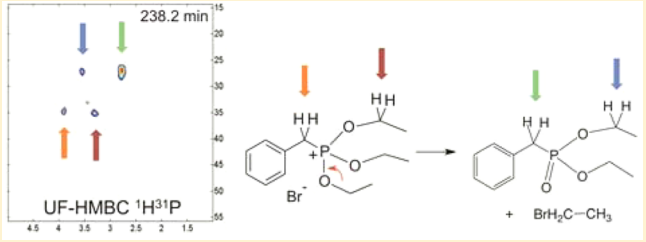

1. INTRODUCTION

Organophosphorus compounds bearing C–P bonds, such as phosphonates, phosphinates and phosphine oxides have found a wide range of useful applications in the important fields of agriculture, medicine, materials science and synthetic chemistry as catalysts and synthetic intermediates.[1] Phosphonates are a key functional group in organic synthesis[2] and biochemistry,[3] particularly in the formation of C–C bonds by Horner–Wadsworth–Emmons reaction, which is a variant of the well-known Wittig–Horner synthesis.[4] Unfortunately, some of these compounds have been also misused as nerve chemical agents.[5]

The Michaelis–Arbuzov reaction[6] has been widely used to obtain a wide range of the required organophosphonates. As shown in Scheme 1, the reaction in its simplest form starts with a trialkyl phosphite **1** and an alkyl halide **2** leading to the formation of a dialkyl alkylphosphonate **3** under elevated temperature conditions. Benzylic and allylic alcohols have also been used as reactants.[7] During this transformation, trivalent phosphorus is converted into a pentavalent phosphorus. In general, a primary alkyl group (CH_2R^4) replaces an alkyl group of the starting phosphite (R^1) forming **3** and a new alkyl halide **4** as side product.

In the absence of a catalyst, the reaction requires high temperature. Moreover, the alkyl halide **4** produced can react with unreacted phosphite, under the same experimental conditions, to reduce the yield of the desired product **3**. For this reason, alternative methods have been developed employing catalysts, such as the Lewis acids $ZnBr_2$ or ZnI_2, that permit the reaction can be carried out at room temperature.[7] In absence of a catalyst, the accepted mechanism consists of two steps: the slow formation of an intermediate **5**, followed by rapid conversion to the phosphonate **3**. The parallel formation of a pentacoordinated intermediate **6** cannot be discarded. When the reaction is catalyzed by halides of Zn, it is not completely clear if the reaction occurs by a S_N2 (as suggested in Scheme 1) or an S_N1 mechanism. Recently, some attempts have been made to provide insight on this point by studying the response to steric effects and the retention and/or loss of stereochemistry.[7] Data obtained from 1D NMR spectra afford only partial and indirect information about the nature of the intermediates that participate in the reaction. Therefore, the use of adequate spectroscopic techniques that enable real-time studies of these dynamic systems is needed. Once again, 2D UF-NMR can provide the opportunity to obtain details of these processes.

Today, ultrafast (UF) 2D NMR[8] is a powerful methodology since it has made possible that the time-consuming acquisition of homonuclear and heteronuclear 2D NMR experiments be carried out in a single scan or in a small number of them. Now 2D NMR can be run at the subsecond scale, opening new areas of analytical application.[9] Studies of dynamic systems in real time can now be carried out with 2D NMR in an increasing number of areas. UF-NMR has taken a prominent role in the study of chemical reactions[10] and biochemical processes,[11] quantitative analysis,[12] biological[13] and biomedical[14] studies as well as in MRI.[15] Additionally, coupling of UF-NMR with other analytical techniques has led to an increasing number of hyphenated approaches, for example with liquid chromatography.[16] The

Received: October 1, 2014
Published: December 5, 2014

Scheme 1

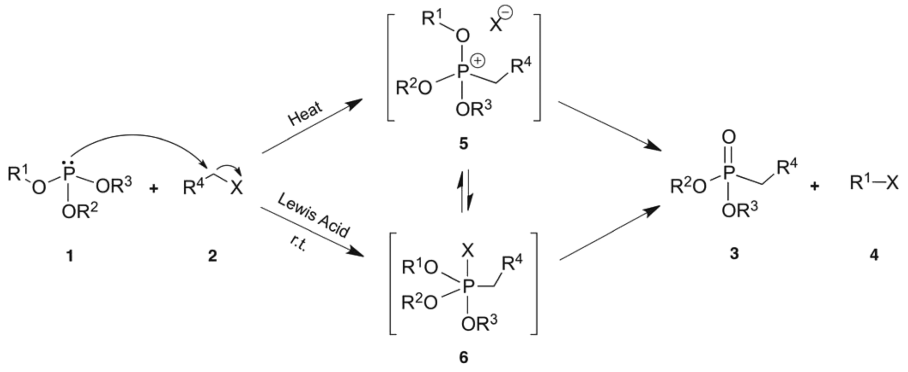

Scheme 2

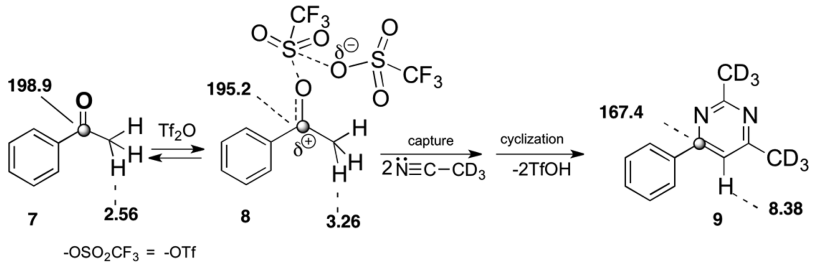

Scheme 3

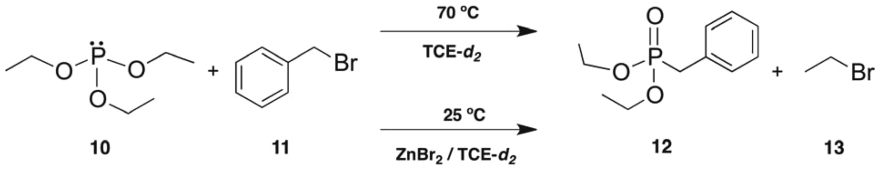

combination with DNP techniques has a clearly promising future.[17]

Real-time NMR measurements have provided unique opportunities to find spectroscopic evidence of mechanistic aspects for known chemical reactions that, in spite of this, have remained open many years. One of these not yet well-known but important systems has been the reaction of ketones with strong electrophiles. To this end, we employed UF-HMBC to study the reaction of ^{13}C-carbonyl-acetophenone (**7**) with trifluoromethanesulfonic acid anhydride (triflic anhydride, Tf_2O) and d_3-acetonitrile, leading to phenylpyrimidine (**9**) (Scheme 2).[10e] The UF sequence consisted of a continuous spatial encoding amplitude modulated UF-HSQC sequence to monitor the evolution of ^2J and $^3J_{HC}$ couplings of 10 Hz. This sequence led to the detection, for the first time, of (trifluoromethylsulfonyloxy)-carbenium ion (**8**) (Scheme 2) from labeled acetophenone **7**. Other nitrilium-salt intermediates were also detected. UF-HMBC provides precise and direct information about the evolution of the carbonyl carbon core along the reaction from starting ketone **7** through intermediate **8** until to the final pyrimidine **9**, by analysis of their ^2J ^{1}H,^{13}C-HMBC detected correlations. However, a detection problem required the use of labeled ^{13}C-carbonyl starting ketone to overcome the low sensitivity of the 2D ^{1}H,^{13}C UF-HMBC sequence.

The present paper deals with the application for the first time of UF-HMBC to study the evolution of the phosphorus core in the Michaelis−Arbuzov reaction. In other words, we will study the conversion of a trivalent P (III) into a pentavalent phosphorus P (V) by ^{1}H,^{31}P UF-HMBC. The range of ^{31}P chemical shifts in diamagnetic compounds extends more than 500 ppm, a wider range than for either carbon and proton. Even small structural differences such as s-orbital character or the electronegativity of its substituents affect the chemical shift and intensity of ^{31}P nucleus markedly, and this can be decisive in monitoring their reactions. Alkyl-trisubstituted phosphite reactants have a range of ^{31}P chemical shifts from 125 to 150 ppm, depending on the electron density on oxygen and therefore of phosphorus.[18] The ^{31}P signals of phosphonate products were expected to appear between approximately 15 and 30 ppm depending on the substitution.[7] A prediction of the position of possible ionic phosphonium salts, formed as intermediates, is difficult; to detect any of these intermediates, a wide range, 10−110 ppm, was selected. Although observable differences in 1D ^{31}P NMR chemical shifts may be large enough to detect different species (reactants and intermediates) present in the reaction, 2D ^{1}H,^{31}P UF-HMBC provides the additional and structural information on the second dimension from the ^{1}H nuclei placed at 1−4 bonds from the ^{31}P nucleus. Both 1D and 2D strategies require similar needs in terms of acquisition time. The ultrafast ^{1}H,^{31}P HMBC sequence should be 150 times more sensitive than the ^{1}H,^{13}C UF-HMBC version and will permit the use of reactants in natural abundance and lower concentrations.

Specifically, we used real-time HMBC ^{1}H,^{31}P-correlations to monitor the reaction of triethyl phosphite (**10**) with benzyl bromide (**11**), which produces diethylbenzyl phosphonate (**12**),

dx.doi.org/10.1021/jo502253p | J. Org. Chem. 2015, 80, 799−805

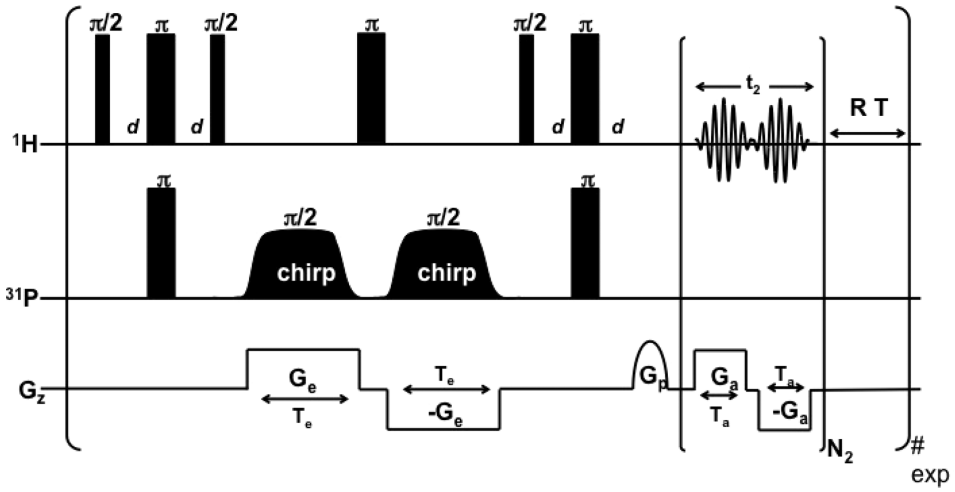

Figure 1. Pulse sequence for the amplitude modulated $^{1}H,^{31}P$ UF-HMBC. The UF-HMBC sequence used is a basic HSQC sequence in which the delay *d* is set to 31.25 ms in order to monitor ^{2}J and $^{3}J_{H,P}$ couplings.

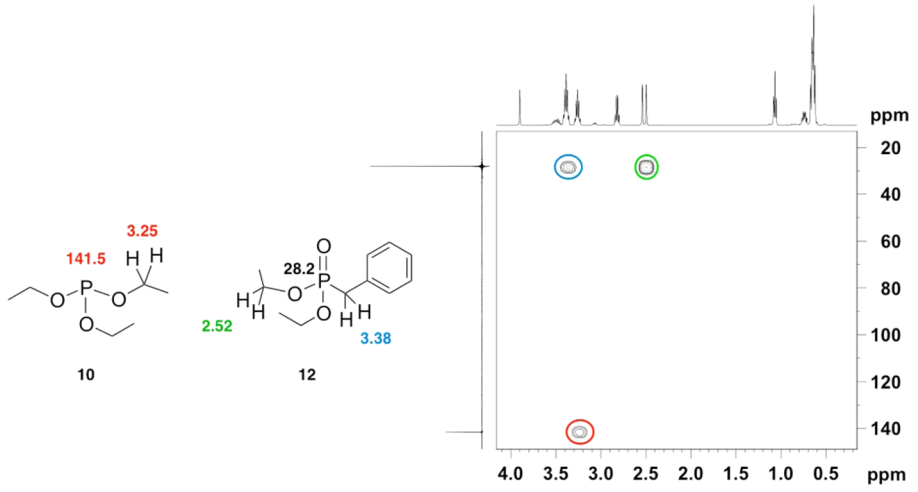

Figure 2. Standard 2D $^{1}H,^{31}P$ HMBC spectrum recorded from a mixture **10**/**12**, obtained after 30 min time for the reaction between triethyl phosphite (**10**) and benzyl bromide (**11**) in 1,1,2,2-tetrachlorethane-d_2 at 343 K, which leads to the diethylbenzyl phosphonate (**12**).

in the absence and the presence of $ZnBr_2$ at various temperatures (Scheme 3).

2. $^{1}H,^{31}P$ UF-HMBC PULSE SEQUENCE FOR FAST MONITORING OF CHEMICAL REACTIONS

The scheme of the $^{1}H,^{31}P$ UF-HMBC pulse sequence is illustrated in Figure 1 and consists basically of a series of amplitude modulated continuous spatial encoding UF-HMBC sequences.[9c] These UF 2D NMR data sets were collected on a Bruker 500 MHz NMR spectrometer using a standard BBO z-gradient probe at 298 K ($ZnBr_2$ present) and 343 K (without $ZnBr_2$). Two different spectral regions **A** and **B** monitored the same aliphatic region: 0.25−4.25 ppm for ^{1}H and two different intervals for ^{31}P: spectral region **A** (−3.0−67.0 ppm) for the formation of the final phosphonate **12** and region **B** (108.9−173.1 ppm), for the evolution of reactant triethylphosphite **10**. Both regions were expected to reveal resonances for possible intermediates and unpredicted products. Both catalyzed and uncatalyzed reactions were monitored in real time by UF-HMBC.

3. RESULTS AND DISCUSSION

3.1. Standard 2D $^{1}H,^{31}P$ HMBC Correlations. A preliminary uncatalyzed reaction was carried out at 343 K to assign signals for the reactants and products by standard 2D $^{1}H,^{31}P$ HMBC. Figure 2 shows the structures and spectra of the starting triethyl phosphite **10** (^{3}J, cross-peaks at 3.25/141.5 ppm, highlighted in red) and final diethylbenzyl phosphonate **12** (^{3}J, 3.38/28.2, blue; 2.52/28.2, ^{2}J, green). Weak signals due to the ^{4}J long-range correlations of methyl groups with P nuclei can also be observed thus indicating the high sensitivity of detection (see the Supporting Information).

3.2. Ultrafast 2D $^{1}H,^{31}P$ HMBC. Analysis in Absence of a Catalyst. *3.2.1. Analysis in Absence of a Catalyst.* The reaction was carried out at 343 K. Acquisition was initiated prior to the injection of benzyl bromide **11**. A total of 112 UF-HMBC spectra were taken in kinetic progression at 10 s delay over 64.90 min (Figure 3).

The spectral ranges established in the preliminary, standard HMBC experiment were used for the UF-HMBC run. Spectra spectra 1, 3, 5, and 7 (range **A**) show the evolution of heteronuclear cross-peaks of the product diethylbenzylphosphonate **12**. Thus, cross-peaks are undetected at the initiation (0

dx.doi.org/10.1021/jo502253p | J. Org. Chem. 2015, 80, 799−805

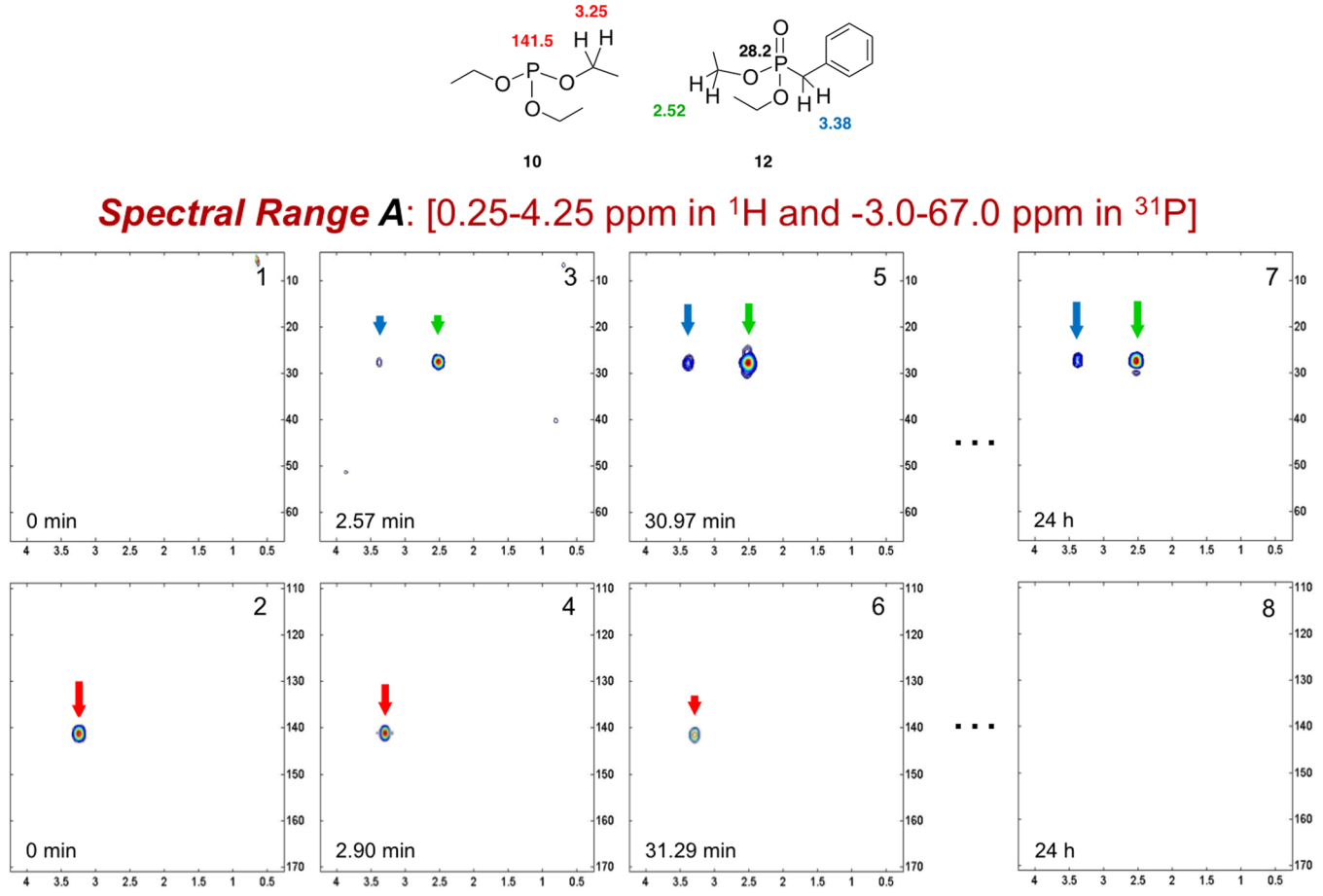

Figure 3. Representative selection of real-time 2D UF-HMBC spectra obtained from the reaction of triethyl phosphite (**10**) and benzyl bromide (**11**) in 1,1,2,2-tetrachlorethane-d_2 at 343 K. Spectra show HMBC cross-peaks from reactant phosphite (red arrows) and product phosphonate (**12**) (green and blue arrows). Top row, spectra 1, 3, 5, and 7 from range A; bottom row, spectra 2, 4, 6, and 8 from range B.

Scheme 4

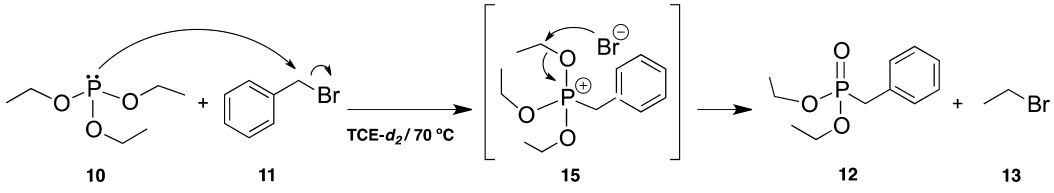

min, spectrum 1) and appear after 2.57 min in spectrum 3 at 3.38/28.2 ppm (blue arrow) and 2.52/28.2 ppm (green arrow). Their intensities rise with reaction time (30.97 min, spectrum 5) and remain apparently constant until the reaction was stopped (24 h, spectrum 7).

The UF-HMBC spectra in Range **B** show the gradual decrease signals for the reactant. Spectra 2, 4, 6, and 8 display cross-peaks from starting triethylphosphite **10** at 3.25/141.5 ppm (red arrow) and its slow decrease to zero over time. Notable is that peaks for intermediates, whose intensity would rise and fall during the reaction, are undetected. Any peaks present would have to be below the intensity of detection that does reveal ^4J long-range correlations of methyl groups with P nuclei. This result is compatible with a bimolecular mechanism S_N2 for the Michaelis–Arbuzov reaction, shown in Scheme 4, in which an ionic intermediate benzyltriethoxy phosphonium bromide would be slowly formed. Its quick evolution leads to the final phosphonate **12**.

3.2.2. Analysis in the Presence of Zinc Bromide as a Catalyst. Figure 4 shows several UF-HMBC consecutive spectra. Here only Range **A** [(1.00–5.00 ppm) for ^{1}H and (14.3–55.7 ppm) for ^{31}P] was examined, since the triethylphosphite **10** complexes with the catalyst zinc bromide and the initial cross-peak at 3.25–141.5 ppm disappear.[7] Because of this, no cross-peaks from reactant were observed. The reaction was carried out at 298 K and a total of 800 2D ^{1}H,^{31}P UF-HMBC spectra were recorded in 273.47 min. In contrast with the uncatalyzed reaction, $ZnBr_2$ accelerates the reaction significantly. This indicates its participation in the determining step of the process.

Selected UF-HMBC (spectra 1, 2, 3, 4 and 5) shows the evolution of the reaction with time. Cross-peaks from final phosphonate **12** (blue and green arrows) are once again present

dx.doi.org/10.1021/jo502253p | J. Org. Chem. 2015, 80, 799–805

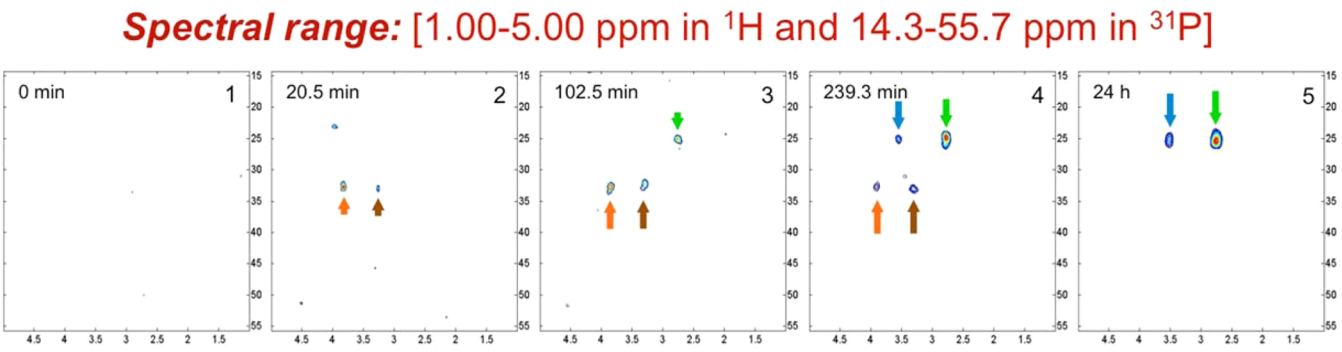

Figure 4. Representative selection of real-time 2D UF-HMBC spectra obtained from the reaction of triethyl phosphite (**10**) with benzyl bromide (**11**) and zinc bromide in 1,1,2,2-tetrachlorethane-d_2 at 298 K. Spectra show HMBC cross-peaks from final phosphonate (**12**) (green and blue arrows) and new cross-peaks (orange and brown arrows) are observed, which belong to the reactive intermediate benzyltriethoxy phosphonium bromide (**15**).

Scheme 5

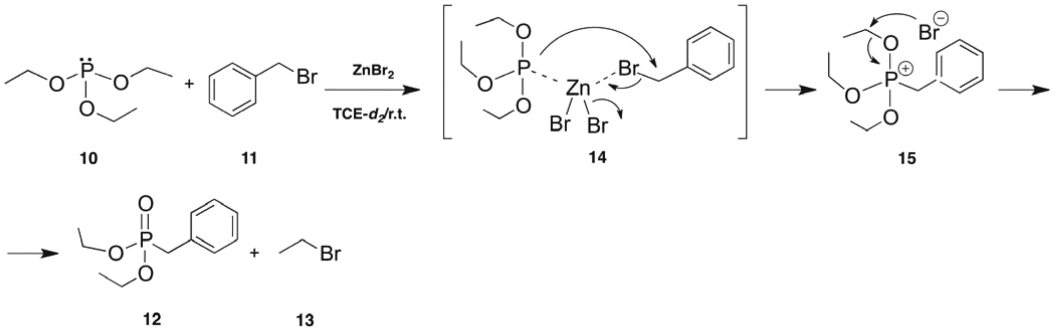

at 102.5 min, but now, new and earlier cross-peaks at 3.90/33.3 ppm and 3.25/33.3 ppm (orange and brown arrows), rise after 20.5 min. Their intensities rise, decrease slowly with the time, and are absent when the reaction was stopped. This behavior indicates a reactive intermediate. No additional signals were detected before or after the spectra shown.

The structure of the detected intermediate belongs in our opinion to the benzyltriethoxy phosphonium bromide **15** (Figure 4). This phosphonium salt formed have enough stability to be detected by the ultrafast HMBC experiment and its structure is in good agreement with the ^{31}P NMR chemical shift of similar isolated analogs.[7a,d,18,19]

The spectroscopic evidence obtained from UF-HMBC and the acceleration observed suggest that the mechanism of the Michaelis–Arbuzov reaction takes place in a stepwise process (Scheme 5). The reaction is initiated by the formation of a zinc complex **14**, which evolves to the ionic adduct intermediate **15**. Unfortunately, additional signals that belong to the complex **14**, in which the Zn atom is present,[7a,b] have not been detected. ^{31}P NMR studies and single crystal X-ray diffraction measurements have confirmed that the adducts-type **15** and other similar intermediates derived from both aryl and alkyl P(III) esters are true phosphonium salts rather than pentacoordinate species.[7c] Decomposition of intermediate **15** would lead to the final phosphonate **12**. Both formation and decomposition steps are balanced making possible a stationary concentration of **15** that therefore enables its observation. The final decomposition or evolution step of the relatively stable intermediate **15** under the experimental thermal conditions should take place through a unimolecular process. According to this and also to the observed racemization, when chiral benzyl bromides were used,[7f] may be proposed an S_N1-type mechanism for the catalyzed by zinc bromide reaction of Michaelis–Arbuzov.

4. CONCLUSIONS

Two-dimensional ^{1}H,^{31}P UF-HMBC is a useful and highly sensitive sequence able to monitor an organic reaction such as the Michaelis–Arbuzov in real time, and to easily obtain direct structural information about the changes produced in the environment of the reaction center (P atom). The methodology can be applied without labeled reactants and has permitted monitoring of the reaction in the absence and in the presence of the catalyst zinc bromide. When the catalyst was used, a relatively stable intermediate benzyltriethoxy phosphonium bromide **15** was detected, whose evolution is in agreement with a unimolecular mechanism. No additional intermediates with metal-containing structures were detected. Further work to extend this methodology to other chemical and biological systems in which the ^{31}P and ^{15}N nuclei are present is in progress.

dx.doi.org/10.1021/jo502253p | J. Org. Chem. 2015, 80, 799–805

5. EXPERIMENTAL SECTION

5.1. Materials and Methods. All starting materials were purchased from commercial suppliers and used without purification. NMR spectra were recorded at 500 MHz. The ^{1}H, ^{13}C, and ^{31}P chemical shifts were reported in parts per million (δ) referenced to residual solvent signals at $\delta_{H/C}$ 5.32/54.0 (1,1,2,2-tetrachloroethane-d_2) relative to tetramethylsilane (TMS) as the internal standard and δ_P 0.00 ppm (85% phosphoric acid in D_2O).

5.2. Monitoring Procedure. A solution of triethyl phosphite in 0.6 mL of 1,1,2,2-tetrachloroethane-d_2 was prepared and added to a 5 mm NMR tube, which was located inside the magnet. Standard NMR (tunning, lock, shiming) and temperature adjustments were carried out before the injection of the benzyl bromide. From outside the spectrometer, the stoichiometric amount of benzyl bromide, dissolved in 1,1,2,2-tetrachloroethane-d_2, was injected into the NMR tube using a fast mixing device, consisting of a long Teflon tube which connected a syringe with a Luer-lock tip to the reaction mixture (see the Supporting Information). The NMR tube was fitted with a cap with a hole and a bearing to minimize oscillations of the injection tube. In the fully loaded position, the injection tube contained, (in order) from the bottom tip upward: an air bubble of ca. 50 μL, the reactant to be added (a solution of benzyl bromide and 1,1,2,2-tetrachloroethane-d_2) and another air bubble (about 100 μL). The upper part of the injection tube was filled with an organic solvent (1,1,2,2-tetrachloroethane-d_2) to efficiently propagate the pressure throughout the mixing device. The bottom end of the injection tube was immersed 1−2 mm in the solution (see the Supporting Information) and well above of the detection coil zone. The vertical position of the NMR tube was adjusted with the tube spinner. Standard NMR (tunning, lock, shiming) and temperature adjustments were carried out before starting the experiment. Acquisitions were started before the injection of the benzyl bromide.

5.3. Monitoring the Reaction of Triethyl Phosphite (10) with Benzyl Bromide (11) by UF-HMBC (in the Absence of $ZnBr_2$). According to the procedure mentioned above, a solution of 31.22 μL (300 mM) of triethyl phosphite **10** in 0.6 mL of 1,1,2,2-tetrachloroethane-d_2 was added to a 5 mm NMR tube, and 21.41 μL (300 mM) of benzyl bromide **11**, dissolved in 0.05 mL of 1,1,2,2-tetrachloroethane-d_2, was injected into the NMR tube.

5.3.1. Acquisition Parameters. The amplitude modulated, continuous spatial encoding ^{1}H,^{31}P UF-HMBC spectra were collected at 343 K. Two different regions **A** and **B** were studied. The region **A** encompasses 0.25−4.25 ppm for ^{1}H and −3.0−67.0 ppm for ^{31}P (every ^{1}H,^{31}P UF-HMBC spectrum taken in 10.32 s). The region **B** encompasses 0.25−4.25 ppm for ^{1}H and 108.9−173.1 ppm for ^{31}P (every ^{1}H,^{31}P UF-HMBC spectrum taken in a longer time of 14.32 s; the reason is that in this window doubled signals from the final product appear and irradiation of them must be done). Two UF-HMBC spectra from regions **A** and **B**, with a delay of 10 s between them, were taken in a total time of 34.64 s. Chirp pulse bandwidth = 40 kHz; encoding gradient strength G_e = 10.70 G cm^{-1}; encoding time t_1^{max} = 5.0 ms; acquisition gradient strength G_a = 40.13 G cm^{-1}; acquisition time T_a = 250 μs; number of acquisition steps N_2 = 64 cycles of ±gradient pairs; gradient switching time = 40 μs. Chirp pulse strength was adjusted to a 90° pulse. A sinusoidal purge gradient of 16.01 G cm^{-1} during 200 μs was applied before acquisition. Time used for INEPT block was 31.25 ms and number of scans NS = 2 (delay = 5 s). A total of 112 ^{1}H,^{31}P UF-HMBC spectra were recorded in 64.90 min.

5.4. Monitoring the Reaction of Triethyl Phosphite (10) with Benzyl Bromide (11), in the Presence of $ZnBr_2$. According to the procedure mentioned above, a solution of 31.22 μL (300 mM) of triethyl phosphite **10** and 35.8 mg (60 mM) of $ZnBr_2$ in 0.6 mL of tetrachloroethane-d_2 was prepared and added to a 5 mm NMR tube. A total of 21.41 μL (300 mM) of benzyl bromide **11** was dissolved in 0.05 mL of tetrachloroethane-d_2 and injected into the NMR tube.

5.4.1. Acquisition Parameters. The amplitude modulated, continuous spatial encoding ^{1}H,^{31}P UF-HMBC spectra were collected at 298 K. The acquired region encompasses 1.00−5.00 ppm for ^{1}H and 14.3−55.7 ppm for ^{31}P (every ^{1}H,^{31}P UF-HMBC spectra taken in 10.51 s). Chirp pulse bandwidth = 40 kHz; encoding gradient strength G_e = 10.70 G cm^{-1}; encoding time t_1^{max} = 5.0 ms; acquisition gradient strength G_a = 26.75 G cm^{-1}; acquisition time T_a = 250 μs; number of acquisition steps N_2 = 64 cycles of ±gradient pairs; gradient switching time = 40 μs. Chirp pulse strength was adjusted to a 90° pulse. A sinusoidal purge gradient of 16.01 G cm^{-1} during 200 μs was applied before acquisition. Time used for INEPT block was 31.25 ms and number of scans NS = 2 (delay = 10 s). A total of 800 ^{1}H,^{31}P UF-HMBC spectra were recorded in 273.47 min.

The calculation of specific acquisition parameters was done using a home-written program in Matlab 7.11.0.584 (MathWorks, USA) and the spectra were acquired using Topspin 1.3. To obtain the 2D NMR spectra from the acquired data, home written routines using Matlab were used.[20] For each acquired data set, an rearrangement of the data followed by a conventional Fourier Transform in the direct dimension is necessary.[8a] Both spectra obtained, one from the data acquired during the positive gradients and the other one from the data acquired during the negative gradients, were added to achieve a higher S/N. For this reason, a small displacement between both spectra must be adjusted before the addition. In these experiments it is not necessary to realign the data before the FT due to a gradient drooping[8b] because this mismatch was compensated during the acquisition. To improve the resolution of the spectra, a conventional zero filling in both direct and indirect, dimensions was performed before the FT. Finally, an apodization with a sinusoidal function was applied in the direct domain in order to improve the resolution and the line shapes. Spectra were represented in magnitude mode.

■ ASSOCIATED CONTENT

Ⓢ Supporting Information

Fast mixing device used in the UF-HMBC experiments. Standard ^{1}H,^{31}P HMBC spectra from reaction mixture registered under different S/N conditions. This material is available free of charge via the Internet at http://pubs.acs.org.

■ AUTHOR INFORMATION

Corresponding Author

*E-mail: aherrera@quim.ucm.es

Notes

The authors declare no competing financial interest.

■ ACKNOWLEDGMENTS

The authors acknowledge financial support from MINECO (Grants CTQ2010-14936). Z.P. acknowledges Universidad Complutense de Madrid for a FPI predoctoral fellowship. We gratefully acknowledge the CAI de RMN y RSE (Universidad Complutense de Madrid) for recording the NMR spectra. We thank also Prof. John Almy for helpful discussions.

■ REFERENCES

(1) (a) Schug, K. A.; Linder, W. *Chem. Rev.* **2005**, *105*, 67−113. (b) Moonen, K.; Laureyn, I.; Stevens, C. V. *Chem. Rev.* **2004**, *104*, 6177−6215. (c) Palacios, F.; Alonso, C.; Santos, J. M. *Curr. Org. Chem.* **2004**, *8*, 1481−1496. (d) Faisca Phillips, A. M. *Mini-Rev. Org. Chem.* **2014**, *11*, 164−185. (e) Tomlin, C.; Turner, J., Ed.; *The Pesticide Manual*, 14th. ed.; British Crop Protection Council: Alton, U.K., 2006.

(2) (a) Guerrero, G.; Alauzun, J. G.; Granier, M.; Laurencin, D.; Mutin, P. H. *J. Chem. Soc., Dalton Trans.* **2013**, *42*, 12569−12585. (b) Engel, R.; Cohen, J. I. *Synthesis of Carbon-Phosphorous Bonds*, 2nd. ed.; CRC Press: Boca Raton, FL, 2004. (c) Vadapalli, C.; Tapas, S.; Atanu, D.; Sakiat, H. *J. Chem. Soc., Dalton Trans.* **2011**, *40*, 5394−5418. (d) Steel, P. G.; Woods, T. M. *Synthesis* **2009**, *22*, 3897−3904. (e) Shimizu, G. K. H.; Vaidhyanathan, R.; Taylor, J. M. *Chem. Soc. Rev.* **2009**, *38*, 1430−1449.

(3) (a) Ju, K.-S.; Doroghazi, J. R.; Metcalf, W. W. *J. Ind. Microbiol. Biotechnol.* **2014**, *41*, 345−356. (b) McGrath, J. W.; Chin, J. P.; Quinn, J. P. *Nat. Rev. Microbiol.* **2013**, *11*, 412−419. (c) Metcalf, W. W.; Van der Donk, W. A. *Annu. Rev. Biochem.* **2009**, *78*, 65−94.

(4) (a) Bisceglia, J. A.; Orelli, L. R. *Curr. Org. Chem.* **2012**, *16*, 2206−2230. (b) Odinets, I. L.; Matveeva, E. V. *Russ. Chem. Rev.* **2012**, *81*, 221−238. (c) Sulzer-Mossé, S.; Alexakis, A.; Mareda, J.; Bollot, G.; Bernardinelli, G.; Filinchunk, Y. *Chem.—Eur. J.* **2009**, *15*, 3204−3220. (d) Maryanoff, B. E.; Reitz, A. B. *Chem. Rev.* **1989**, *89*, 863−927.

(5) (a) Kim, K.; Tsay, O. G.; Atwood, D. A.; Churchill, D. G. *Chem. Rev.* **2011**, *111*, 5345−5403. (b) *Convention on the Prohibition of the Development, Production, Stockpiling and Use of Chemical Weapons and on Their Destruction*; Technical Secretariat of the Organization for the Prohibition of Chemical Weapons: The Hague, Netherlands, 2014.

(6) (a) Michaelis, A.; Kaehne, R. *Chem. Rev.* **1898**, *31*, 1048−1058. (b) Gerrard, W.; Green, W. J. *J. Chem. Soc.* **1951**, 2550−2553. (c) Garner, A. Y.; Chapin, E. C.; Scanlon, P. M. *J. Org. Chem.* **1959**, *24*, 532−536. (d) Arbuzov, B. A. *Pure Appl. Chem.* **1964**, *9*, 315−370. (e) Hartley, F. H., Ed.; *The Chemistry of Organophosphorus Compounds*; Wiley: New York, 1996. (f) Bhattacharya, A. K.; Thyagarajan, G. *Chem. Rev.* **1981**, *81*, 415−430.

(7) (a) Richardson, R. M.; Barney, R. J.; Wiemer, D. F. *Tetrahedron Lett.* **2012**, *53*, 6682−6684. (b) Barney, R. J.; Richardson, R. M.; Wiemer, D. F. *J. Org. Chem.* **2011**, *76*, 2875−2879. (c) Hudson, H. R.; Powroznyk, L. *ARKIVOC* **2004**, *ix*, 19−33. (d) Hudson, H. R.; Qureshi, A. R. *Polish J. Chem.* **2005**, *79*, 473−480. (e) Colle, K. S.; Lewis, E. S. *J. Org. Chem.* **1978**, *43*, 571−574. (f) Rajeshwaran, G. G.; Nandakumar, M.; Sureshbabu, R.; Mohanakrishnan, A. K. *Org. Lett.* **2011**, *13*, 1270−1273.

(8) (a) Frydman, L.; Scherf, T.; Lupulescu, A. *Prod. Natl. Acad. Sci. U.S.A.* **2002**, *99*, 15858−62. (b) Frydman, L.; Lupulescu, A.; Scherf, T. *J. Am. Chem. Soc.* **2003**, *125*, 9204−9217. (c) Tal, A.; Frydman, L. *Prog. Nucl. Magn. Reson. Spectrosc.* **2010**, *57*, 241−292. (d) Gal, M.; Frydman, L. *Multidimensional NMR Methods for the Solution State*; John Wiley&Sons: Chichester, U.K., 2010; pp 43−60.

(9) (a) Giraudeau, P.; Frydman, L. *Annu. Rev. Anal. Chem.* **2014**, *7*, 129−161. (b) Mishkovsky, M.; Frydman, L. *Annu. Rev. Phys. Chem.* **2009**, *60*, 429−448. (c) Shrot, Y.; Frydman, L. *J. Chem. Phys.* **2008**, *128*, 052209/1−052209/14.

(10) (a) Shapira, B.; Frydman, L. *J. Magn. Reson.* **2003**, *165*, 320−324. (b) Gal, M.; Mishkovsky, M.; Frydman, L. *J. Am. Chem. Soc.* **2006**, *128*, 951−956. (c) Herrera, A.; Fernández-Valle, E.; Martínez-Álvarez, R.; Molero, D.; Pardo, Z. D.; Sáez, R. E.; Gal, M. *Angew. Chem., Int. Ed.* **2009**, *48*, 6274−6277. (d) Pardo, Z. D.; Olsen, G. L.; Fernández-Valle, M. E.; Frydman, L.; Martínez-Álvarez, R.; Herrera, A. *J. Am. Chem. Soc.* **2012**, *134*, 2706−2715. (e) Herrera, A.; Fernández-Valle, M. E.; Gutiérrez, E. M.; Martínez-Álvarez, R.; Molero, D.; Pardo, Z. D.; Sáez, E. *Org. Lett.* **2010**, *12*, 144−147. (f) Giraudeau, P.; Lemeunier, P.; Coutand, M.; Doux, J. M.; Gilbert, A.; Remaud, G. S.; Akoka, S. *J. Spectrosc. Dyn.* **2011**, *1*, 2. (g) Queiroz, L. H. K., Jr; Giraudeau, P.; dos Santos, E. A. B.; Oliveira, K. T.; Ferreira, A. G. *Magn. Reson. Chem.* **2012**, *50*, 496−501. (h) Fernández, I.; Fernández-Valle, M. E.; Martínez-Álvarez, R.; Molero-Vílchez, D.; Pardo, Z. D.; Sáez-Barajas, E.; Sánchez, A.; Herrera, A. *J. Org. Chem.* **2014**, *79*, 8086−8093.

(11) (a) Gal, M.; Schanda, P.; Brutscher, B.; Frydman, L. *J. Am. Chem. Soc.* **2007**, *129*, 1372−1377. (b) Lee, M.-K.; Gal, M.; Frydman, L. *Proc. Natl. Acad. Sci. U.S.A.* **2010**, *105*, 9192−9197.

(12) (a) Giraudeau, P.; Akoka, S. *Adv. Bot. Res.* **2013**, *67*, 99−158. (b) Giraudeau, P.; Remaud, G. S.; Akoka, S. *Anal. Chem.* **2009**, *81*, 479−484. (c) Pathan, M.; Akoka, S.; Tea, I.; Charrier, B.; Giraudeau, P. *Analyst* **2011**, *136*, 3157−3163. (d) Le Guennec, A.; Tea, I.; Antheaume, I.; Martineau, E.; Charrier, B.; Pathan, M.; Akoka, S.; Giraudeau, P. *Anal. Chem.* **2012**, *84*, 10831−10837.

(13) (a) Giraudeau, P.; Massou, S.; Robin, Y.; Cahoreau, E.; Portais, J.-C.; Akoka, S. *Anal. Chem.* **2011**, *83*, 3112−3119. (b) Pathan, S.; Akoka, S.; Giraudeau, P. *J. Magn. Reson.* **2012**, *214*, 335−339.

(14) Martineau, E.; Tea, I.; Akoka, S.; Giraudeau, P. *NMR Biomed.* **2012**, *25*, 985−992.

(15) (a) Tal, A.; Frydman, L. *J. Magn. Reson.* **2007**, *189*, 46−58. (b) Ben-Eliezer, N.; Goerke, U.; Ugurbil, K.; Frydman, L. *Magn. Reson. Imag.* **2012**, *30*, 1401−1408. (c) Schmidt, R.; Baishya, B.; Ben-Eliezer, N.; Seginer, A.; Frydman, L. *Magn. Reson. Imaging* **2014**, *32*, 60−70. (d) Schmidt, R.; Laustsen, C.; Dumez, J.-N.; Kettunen, M. I.; Serrao, E. M.; Marco-Rius, I.; Brindle, K. M.; Ardenkjaer-Larsen, J. H.; Frydman, L. *J. Magn. Reson.* **2014**, *240*, 8−15.

(16) (a) Shapira, B.; Karton, A.; Aronzon, D.; Frydman, L. *J. Am. Chem. Soc.* **2004**, *126*, 1262−1265. (b) Queiroz Júnior, L. H. K.; Queiroz, D. P. K.; Dhooghe, L.; Ferreira, A. G.; Giraudeau, P. *Analyst* **2012**, *137*, 2357−2361.

(17) (a) Frydman, L.; Blazina, D. *Nat. Phys.* **2007**, *3*, 415−419. (b) Mishkovsky, M.; Frydman, L. *ChemPhysChem* **2008**, *9*, 2340−2348. (c) Giraudeau, P.; Shrot, Y.; Frydman, L. *J. Am. Chem. Soc.* **2009**, *131*, 13902−13903.

(18) (a) Kühl, O. *Phosphoros-31 NMR Spectroscopy*; Springer: Greifswald, Germany, 2008. (b) Berger, S.; Braun, S.; Kalinowski, H. O. *NMR Spectroscopy of the Non-Metallic Elements*; John Wiley&Sons: Chichester, England, 1997.

(19) Colle, K. S.; Lewis, E. S. *J. Org. Chem.* **1978**, *43*, 571−574.

(20) Fernández-Valle, E.; Ph.D. Dissertation, Universidad Complutense, 2013. Routines and programs used can be downloaded from: http://eprints.ucm.es/23718/.